Synthesis Imaging in Radio Astronomy II
ASP Conference Series, Vol. 180, 1999
G. B. Taylor, C. L. Carilli, and R. A. Perley (eds.)

18. Bandwidth and Time-Average Smearing

A. H. Bridle & F. R. Schwab
National Radio Astronomy Observatory, Charlottesville, VA 22903, U.S.A.

Abstract.
This is the first of three lectures to deal with problems in imaging wide fields-of-view. Its goal is to quantify the first two effects described in Lecture 17—bandwidth smearing and time-average smearing. Both effects cause the synthesized image to be distorted in ways that cannot adequately be described (except locally) as a convolution of the true sky brightness distribution with a spatially invariant point source response function. Rather, the degree of smearing is a function of angular distance from the delay-tracking center (for bandwidth smearing) or the phase-tracking center (for time-average smearing). The effects therefore persist after simple (position-independent) deconvolution with methods like 'CLEAN' or MEM. Since these distortions cannot be remedied by calibration (or self-calibration), it is important to devise synthesis observing strategies that hold the distortions down to acceptable levels. We wish now to characterize the two effects mathematically and to justify the approximations embodied in the practical formulae used elsewhere.

1. Bandwidth Smearing (Chromatic Aberration)

1.1. General description of the effect

In Lecture 1, the basic Fourier transform relation between the *monochromatic* visibilities V_ν and the *monochromatic* intensity distribution I_ν was given in Equation 1–9:

$$I_\nu(l,m) = \int_{-\infty}^{\infty}\int_{-\infty}^{\infty} V_\nu(u,v)e^{2\pi i(ul+vm)}\,du\,dv\,. \qquad (18\text{–}1)$$

In practice, although the receiver passbands are of finite width $\Delta\nu > 0$, we treat all the visibility data as though they correspond to measurements at a single central frequency, ν_0. To see how this distorts the synthesized image, consider an infinitesimal bandwidth $d\nu$ centered on frequency ν. The actual spatial frequency coordinates of a visibility for frequency ν are, let us say, (u_ν, v_ν). But when handling the data, we instead assign the frequency-independent coordinates $u_0 = \frac{\nu_0}{\nu}u_\nu$ and $v_0 = \frac{\nu_0}{\nu}v_\nu$, as though all the data had been taken at frequency ν_0. Within any given visibility sample, the data from all incremental bandwidths $d\nu$ within the passband $\Delta\nu$ are averaged, with weights determined by the instrumental passband shape, and are assigned the *same* u_0 and v_0.

How does this *imprecision* in our handling of the (u,v) coordinates affect the computed brightness distribution? We can answer this by using the *similarity theorem* of Bracewell (1978), which states (see also Lecture 7) that if the functions $X(\mathbf{x})$ and $x(\mathbf{u})$ form a Fourier transform pair in n dimensions, i.e., if $X = \mathfrak{F}x$, then rescaling the coordinates in one domain by a factor α corresponds to rescaling the transform in the other domain by the reciprocal scale factor $1/\alpha$, and renormalizing the amplitudes, so that

$$\frac{1}{|\alpha|^n}X\left(\frac{\mathbf{x}}{\alpha}\right) = \mathfrak{F}x(\alpha\mathbf{u})\,. \qquad (18\text{–}2)$$

In our case, $n = 2$, $\alpha = \nu_0/\nu$, X is to be identified with I, and x with V.

How does the passband *shape* affect the result? In the general case, the i^{th} antenna and its associated electronics would be described by a voltage bandpass characteristic $g_i(\nu')$, where $\nu' = \nu - \nu_0$. The power bandpass of the i–j interferometer pair in an array would then be $G_{i,j}(\nu') = g_i(\nu')g_j^*(\nu')$. We will assume, however, that all antennas and electronic systems are identical, so that the whole array is characterized by a single power bandpass function $G(\nu')$. In this case, which is a major design goal for nearly every synthesis array, the effect of the passband shape can be described by a multiplication in the (u, v) plane, as we now show.

First we rewrite Equation 18–1 in terms of the *bandwidth-smeared* intensity $\widetilde{I}(l, m)$ and the *frequency-dependent* u's and v's:

$$\widetilde{I}(l,m) = \int_{-\infty}^{\infty}\int_{-\infty}^{\infty} \widetilde{V}(u_0, v_0) e^{2\pi i(u_0 l + v_0 m)}\, du_0\, dv_0\,, \tag{18–3}$$

where the smeared visibilities $\widetilde{V}$ are obtained from the true V's by rescaling, weighting by the passband function $G(\nu')$ and then summing over all infinitesimal bandpasses $d\nu$. In summing the visibilities over frequency, we must take a further important effect into account. The delay-tracking is appropriate to the center of the field-of-view and the center frequency ν_0. For signals at frequency ν arriving from a direction (l, m) at the interferometer with spatial frequency (u_0, v_0), the inserted delay is in error by an amount $\tau = (u_0 l + v_0 m)/\nu_0$, so the phase is shifted by $2\pi(\nu - \nu_0)\tau = 2\pi\nu'(u_0 l + v_0 m)/\nu_0$. The expression for the smeared visibility is therefore

$$\widetilde{V}(u_0, v_0) = \frac{1}{\int_{-\infty}^{\infty} G(\nu')\, d\nu'} \int_{-\infty}^{\infty} V\left(u_0\frac{\nu}{\nu_0}, v_0\frac{\nu}{\nu_0}\right)\left(\frac{\nu}{\nu_0}\right)^2 G(\nu') e^{2\pi i\frac{\nu'}{\nu_0}(u_0 l + v_0 m)}\, d\nu'\,. \tag{18–4}$$

Now consider the bandwidth smearing of a point source with unit amplitude. As Equation 18–4 describes averaging the visibilities V along a *radius* in the (u, v) plane, we can choose a source on the l-axis, at $(l_0, 0)$, with no loss of generality. Using the *shift theorem* for Fourier transforms (Bracewell 1978), the true visibility is

$$V(u,v) = e^{-2\pi i u l_0}\,. \tag{18–5}$$

The array measures this at points described by the sampling function $S(u_0, v_0)$, and the data are multiplied by a weighting function $W(u_0, v_0)$ when making the image (see Sec. 2.2 of Lecture 7). Inserting the sampled and weighted point source visibility into Equation 18–4,

$$\widetilde{V}(u_0, v_0) = \int_{-\infty}^{\infty} S(u_0, v_0) W(u_0, v_0) e^{-2\pi i u_0 \frac{\nu}{\nu_0} l_0}\left(\frac{\nu}{\nu_0}\right)^2 G_n(\nu') e^{2\pi i\frac{\nu'}{\nu_0}(u_0 l + v_0 m)}\, d\nu'\,, \tag{18–6}$$

where $G_n(\nu')$ is the *normalized* passband function $G(\nu')/\int_{-\infty}^{\infty} G(\nu')\, d\nu'$. If the fractional bandwidth is sufficiently small, we can put $(\nu/\nu_0)^2 = 1$. Equation 18–3 for the bandwidth-smeared intensity can then be written as

$$\widetilde{I}(l,m) = \int_{-\infty}^{\infty}\left[\int_{-\infty}^{\infty} S(u_0,v_0)W(u_0,v_0)e^{-2\pi i u_0 \frac{\nu}{\nu_0} l_0} G_n(\nu')e^{2\pi i u_0 \frac{\nu'}{\nu_0} l}\, d\nu'\right] e^{2\pi i u_0 l}\, du_0\, \delta(m). \quad (18\text{–}7)$$

Rearranging the exponentials, we can rewrite Equation 18–8 as

$$\widetilde{I}(l,m) = \int_{-\infty}^{\infty} S(u_0,v_0)W(u_0,v_0)e^{2\pi i u_0 (l-l_0)}\left[\int_{-\infty}^{\infty} G_n(\nu')e^{2\pi i u_0 \frac{\nu'}{\nu_0}(l-l_0)} d\nu'\right] du_0\, \delta(m)\,. \quad (18\text{–}8)$$

This is an interesting form for $\widetilde{I}$—the term in square brackets is the Fourier transform over ν' of the normalized passband function, to an argument that is the delay $\tau = \frac{u_0}{\nu_0}(l - l_0)$ corresponding to position offset $l - l_0$. It is therefore useful to define a *delay function* $d(\tau)$ related to the passband function $G(\nu')$ by

$$d(\tau) = \frac{1}{\int_{-\infty}^{\infty} G(\nu')\, d\nu'} \int_{-\infty}^{\infty} G(\nu')e^{2\pi i \tau \nu'}\, d\nu'\,. \quad (18\text{–}9)$$

The effect of finite bandwidth on the measured visibilities can be described as multiplying the true visibilities by this delay function, which depends on both u_0 and $l - l_0$.

Notice also that Equation 18–9 shows that $\widetilde{I}(l)$ is the Fourier transform over u_0 of the product of four functions—the sampling function $S(u_0, v_0)$, the weighting function $W(u_0, v_0)$, the pristine visibility function $e^{-2\pi i u_0 l_0}$, and the delay function $d(\tau)$. Equation 18–9 can therefore be rewritten, using the convolution theorem, as the convolution of four transforms:

$$\widetilde{I}(l,m) = \mathfrak{F}S * \mathfrak{F}W * \int_{-\infty}^{\infty} e^{2\pi i u_0 (l-l_0)} du_0\, \delta(m) * \int_{-\infty}^{\infty} d(\tau)e^{2\pi i u_0 l} du_0\,. \quad (18\text{–}10)$$

The first two convolutions give us the narrow-band image—a "dirty beam" $B = \mathfrak{F}S * \mathfrak{F}W$ centered on $(l_0, 0)$. The third is a convolution with a *position-dependent* function that we will call the bandwidth *distortion function* $D(l)$. This distortion function is the Fourier transform over u_0 of the delay function $d(\tau)$. Unlike the dirty beam B, the width and amplitude of D vary with radial distance l_0 from the delay center. Furthermore, D is always oriented along the radius to the delay center. The final image $\widetilde{I}$ is therefore a simple, position-independent, convolution $\mathfrak{F}S * \mathfrak{F}W * I * D$ *only* in the trivial case of a single point source I. The bandwidth distortion of an extended image can be thought of as a "radially-dependent convolution".

The above analysis shows that the bandwidth effect can be characterized by three related functions, the (power) *passband function* $G(\nu')$, the *delay function* $d(\tau)$ and the one-dimensional (radial) *distortion function* $D(l)$. We now give explicit forms of these functions, and derive the final "point source response", in a few simple cases. In what follows, we emphasize the radial symmetry by replacing the coordinate l with the radial coordinate $\theta = \sqrt{l^2 + m^2}$ where appropriate.

Just for a moment, let us explicitly include the dependence of the distortion function D on two radial coordinates, θ and θ_0. Then Equation 18–10, expressing

the bandwidth smearing effect on the synthesized image $\widetilde{I}$ *locally* as a convolution of four functions, can be recast in a more general form—valid for the entire image—

$$\widetilde{I}(l,m) = \int_0^\infty (B * I)\left(\frac{l\theta_0}{\sqrt{l^2+m^2}}, \frac{m\theta_0}{\sqrt{l^2+m^2}}\right) D(\sqrt{l^2+m^2}-\theta_0, \theta_0)\, d\theta_0 .$$

If $D(\theta, \theta_0)$ had no dependence on θ_0, then Equation 18–10 would reduce to a convolution equation, since the distortion function appearing in the above equation would be a function solely of the difference $\theta - \theta_0$.

1.2. Square bandpass, no tapering, square (u,v) coverage

This is the case that was used to illustrate bandwidth smearing in Lecture 17 (see Fig. 17–2).

Passband function:

$$G(\nu') = \begin{cases} 1, & \text{if } |\nu'| < \Delta\nu/2, \\ 0, & \text{otherwise}, \end{cases} \qquad \text{thus} \quad \int_{-\infty}^{\infty} G(\nu')\, d\nu' = \Delta\nu . \tag{18–11}$$

Delay function:

$$d(\tau) = \text{sinc}\, \frac{\Delta\nu\,(l_0 u + m_0 v)}{\nu_0} . \tag{18–12}$$

Distortion function:

$$D(\theta) = \frac{\nu_0}{\Delta\nu\,\theta_0}\Pi\left(\frac{\nu_0\theta}{\Delta\nu\,\theta_0}\right), \qquad \text{where} \quad \Pi(s) \equiv \begin{cases} 1, & \text{if } |s| < \frac{1}{2}, \\ 0, & \text{otherwise}. \end{cases} \tag{18–13}$$

Note that the *width* of this distortion function increases as $\Delta\nu\,\theta_0$, whereas its amplitude decreases as $1/(\Delta\nu\,\theta_0)$. This illustrates the principal characteristics of the bandwidth distortion—reduction in amplitude, and radial broadening, of the point source response. It also illustrates that the two effects preserve the *integrated* flux density of the distorted response.

Sampling function:

$$S(u,v) = \Pi(u/A)\,\Pi(v/A) \tag{18–14}$$

(i.e., a filled square of side A, with longest baseline $= A/\sqrt{2}$).

Weighting function:

$$W(u,v) = 1 \quad \text{(uniform weighting)}.$$

Dirty beam:

$$B(l,m) = \text{sinc}\, Al\, \text{sinc}\, Am \tag{18–15}$$

The smeared point source response is B_D, the convolution of the dirty beam B (Eq. 18–15) with the distortion function D (Eq. 18–13). At any given offset $\Delta\theta$ from the beam center at θ_0, the amplitude of this response is

$$\begin{aligned} B_D(\Delta\theta, \theta_0) &= \frac{\nu_0}{\Delta\nu\,\theta_0}\int_{\Delta\theta-\frac{\Delta\nu\,\theta_0}{2\nu_0}}^{\Delta\theta+\frac{\Delta\nu\,\theta_0}{2\nu_0}} \text{sinc}\, A\theta\, d\theta \qquad (18–16) \\ &= \frac{\nu_0}{\pi A \Delta\nu\,\theta_0}\left[\text{Si}\left(\pi A(\Delta\theta + \frac{\Delta\nu\,\theta_0}{2\nu_0})\right) - \text{Si}\left(\pi A(\Delta\theta - \frac{\Delta\nu\,\theta_0}{2\nu_0})\right)\right], \end{aligned}$$

where $\mathrm{Si}(x) \equiv \int_0^x \frac{\sin t}{t}\,dt$ is the sine integral, a standard special function. The HPBW of sinc $A\theta$ is $\theta_{\mathrm{HPBW}} = 1.206/A$. Defining

$$\begin{aligned} \eta &= \pi A \theta_{\mathrm{HPBW}} = 3.79\,, \\ \alpha &= \frac{\Delta\theta}{\theta_{\mathrm{HPBW}}} = \text{offset from peak response in undistorted HPBW's, and} \\ \beta &= \frac{\Delta\nu}{\nu_0}\frac{\theta_0}{\theta_{\mathrm{HPBW}}} = \text{fractional bandwidth } \times \text{ radius in HPBW's,} \end{aligned} \tag{18–17}$$

we can rewrite Equation 18–17 to get the following expression for the degraded beam shape $B_D = B * D$ as a function of offset $\Delta\theta$ from the peak response at θ_0 from the delay center,

$$B_D(\Delta\theta, \theta_0) = \frac{1}{\eta\beta}\left(\mathrm{Si}\,\eta(\alpha + \frac{\beta}{2}) - \mathrm{Si}\,\eta(\alpha - \frac{\beta}{2})\right). \tag{18–18}$$

The peak I of the degraded response to the point source is evaluated by setting $\Delta\theta = 0$, so that α is zero, and substituting into Equation 18–18. The fractional reduction in amplitude of the point source due to bandwidth smearing, $R_{\Delta\nu}$ is the ratio I/I_0, where I_0 is the peak response for $\Delta\nu = 0$ (Eq. 18–18 with $\alpha = 0$ and $\beta = 0$). For this case,

$$R_{\Delta\nu} = \frac{I}{I_0} = \frac{2}{\eta\beta}\mathrm{Si}\frac{\eta\beta}{2}. \tag{18–19}$$

1.3. Square bandpass, circular Gaussian tapering

For this case, the bandpass, delay and distortion functions are identical to those in the previous example (Eqs. 18–11 through 18–13).

Sampling function:

$$S(u,v) = 1 \quad \text{(over an area large relative to the scale of the taper).} \tag{18–20}$$

Weighting (tapering) function:

$$W(u,v) = \frac{\sqrt{\pi}\,\theta_{\mathrm{HPBW}}}{\gamma}\exp\frac{-\pi^2\theta^2_{\mathrm{HPBW}}(u^2+v^2)}{\gamma^2}, \quad (\gamma \equiv 2\sqrt{\ln 2} = 1.665)\,. \tag{18–21}$$

Dirty beam:

$$B(\theta) = \exp\frac{-\gamma^2\theta^2}{\theta^2_{\mathrm{HPBW}}}. \tag{18–22}$$

The calculation of the degraded beam follows that in Section 1.2, leading to

$$B_D(\Delta\theta, \theta_0) = \frac{\sqrt{\pi}}{2\gamma\beta}\left(\mathrm{erf}\gamma(\alpha + \frac{\beta}{2}) - \mathrm{erf}\gamma(\alpha - \frac{\beta}{2})\right), \tag{18–23}$$

where erf is the usual error function. The reduction in amplitude of a point source relative to zero bandwidth is therefore

$$R_{\Delta\nu} = \frac{I}{I_0} = \frac{\sqrt{\pi}}{\gamma\beta}\mathrm{erf}\frac{\gamma\beta}{2}. \tag{18–24}$$

1.4. Gaussian bandpass, circular Gaussian tapering

Passband function:

$$G(\nu') = \exp \frac{-\gamma^2 \nu'^2}{(\Delta\nu)^2}, \quad \text{where } \gamma \equiv 2\sqrt{\ln 2} = 1.665\,, \text{thus } \int_{-\infty}^{\infty} G(\nu')\,d\nu' = \frac{\sqrt{\pi}\,\Delta\nu}{\gamma}. \tag{18–25}$$

Delay function:

$$d(\tau) = \exp \frac{-\pi^2(\Delta\nu)^2(l_0 u + m_0 v)^2}{\gamma^2 \nu_0^2}. \tag{18–26}$$

Distortion function:

$$D(\theta) = \frac{\gamma\nu_0}{\sqrt{\pi}\,\Delta\nu\,\theta_0} \exp \frac{-\gamma^2\nu_0^2\theta^2}{(\Delta\nu)^2\theta_0^2}. \tag{18–27}$$

For this case, the sampling function is again unity, the weighting function is the Gaussian specified by Equation 18–21, and the dirty beam is the Gaussian specified by Equation 18–22. The degraded beam is

$$B_D(\Delta\theta, \theta_0) = \frac{1}{\sqrt{1+\beta^2}} \exp \frac{-\alpha^2\gamma^2}{1+\beta^2}, \tag{18–28}$$

and the reduction in the peak response is

$$R_{\Delta\nu} = \frac{I}{I_0} = \frac{1}{\sqrt{1+\beta^2}}. \tag{18–29}$$

1.5. Graphs of the main bandwidth smearing effects

Figures 18–1 and 18–2, adapted from Perley (1981a), show how the two main effects of bandwidth smearing vary as functions of the dimensionless parameter $\beta = \frac{\Delta\nu}{\nu_0}\frac{\theta_0}{\theta_{\mathrm{HPBW}}}$, for each of the three combinations of band shape and tapering discussed above. The three curves are strikingly similar. When plotted in this way, the variations in undegraded beamwidth due to different (u, v) coverage and tapering are absorbed into the ratio β, emphasizing the utility of this parameter when describing the bandwidth effect.

Note however that the definition of β obscures the true frequency dependence of the bandwidth effect for a *given* synthesis array. Equation 18–9 shows that, for a given array, the delay function depends only on the shape of the passband, not on the observing frequency. The center frequency ν_0 appears in the definition of β only because it multiplies θ_{HPBW} in the denominator. The product $\nu_0\theta_{\mathrm{HPBW}}$ is independent of frequency for a given array. Despite this, it is convenient in practice to factor β in this way.

2. Time-Average Smearing

2.1. General description of the effect

Averaging of the visibility data is another cause of image smearing. Assuming an averaging time τ_a, these averaged data from each correlator are assigned (u, v)

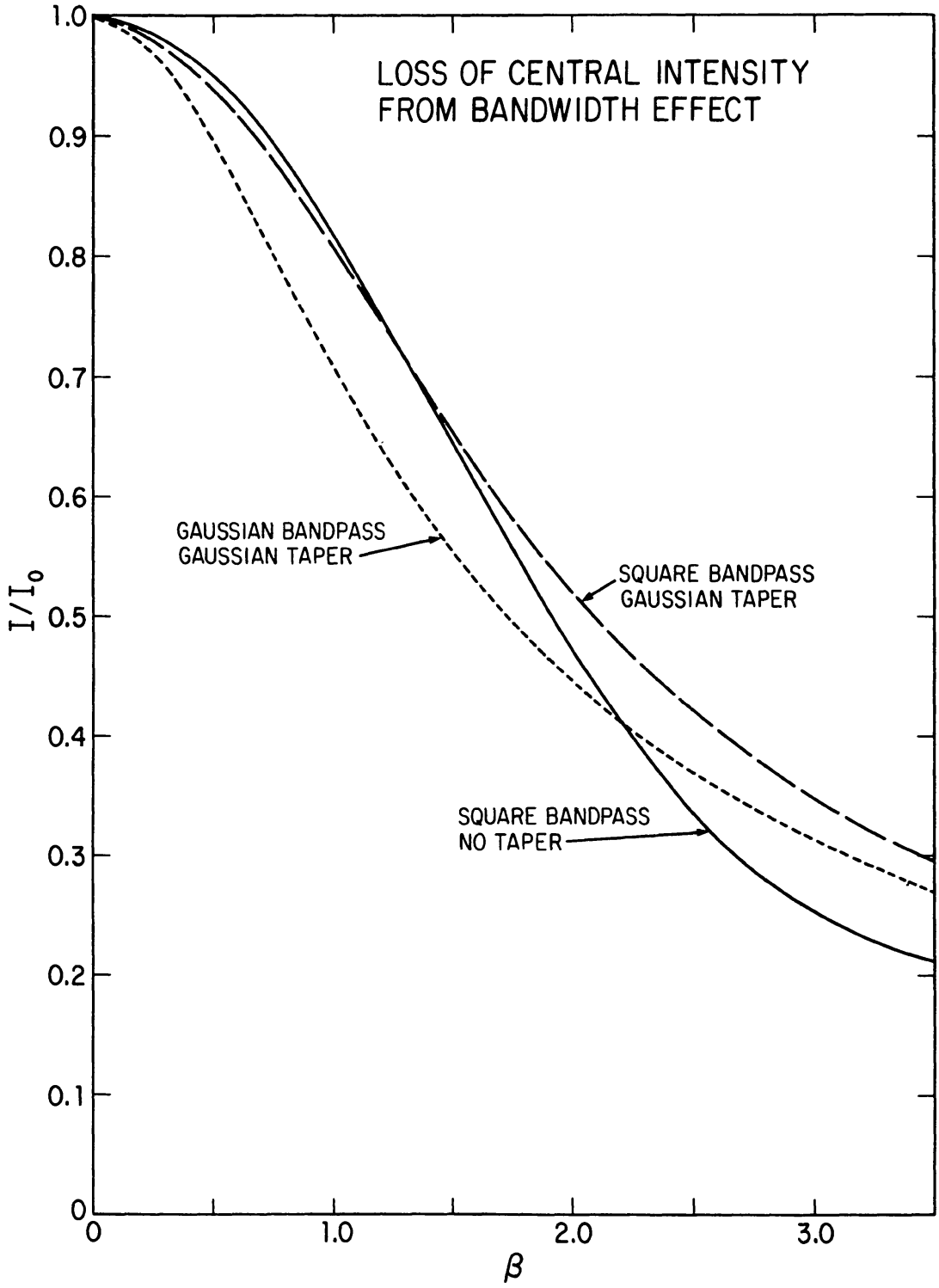

Figure 18–1. The reduction in peak response to a point source, I/I_0, for each of the band shape and taper combinations discussed in Sections 1.2 through 1.4, plotted as a function of the dimensionless parameter β.

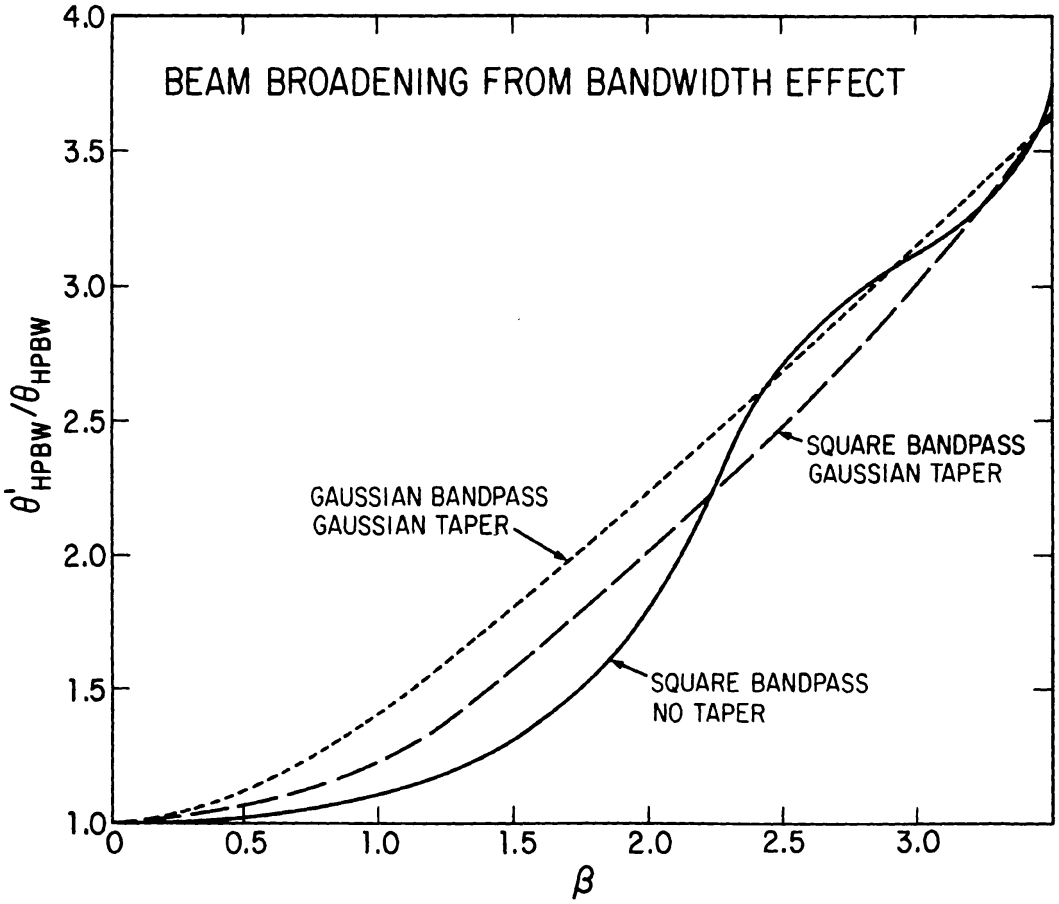

Figure 18–2. The broadening of the point source response relative to zero bandwidth, for each of the band shape and taper combinations discussed in Sections 1.2 through 1.4, plotted as a function of the dimensionless parameter β.

values corresponding to the mid-points t of the averaging intervals, although the data come from time ranges $|\delta t| \leq \tau_a/2$ centered about these mid-points.

For a source at the North or South Celestial Pole, the sampling function is confined to a set of concentric circles in the (u, v) plane, generated by rotating the spacing vector at the Earth's rotational angular velocity ω_e (7.27×10^{-5} rad sec^{-1}). A time offset δt in the assignment of u and v would correspond in this case to a rotation of the visibility function through an angle $\omega_e \delta t$. This would cause the image to be rotated through the same angle, since the Fourier transform commutes with rotations (see Sec. 4.1 of Lecture 7). For an image centered on one of the celestial poles, the effect of time averaging is therefore equivalent to averaging a series of images that are aligned at the l-m origin but have angular offsets up to $\pm\omega_e\tau_a/2$. The weights of the different images in this average reflect the weights of the corresponding times in the time-averaging function. In this particular case, the time-average smearing is therefore equivalent to a distorted *azimuthal* convolution, with a "convolving" function whose shape is determined by the time-averaging function and whose width increases with radius, $\sqrt{l^2 + m^2}$. At the poles, time-average smearing therefore bears an interesting similarity to bandwidth smearing, which produces a distorted *radial*

convolution. The general case is, unfortunately, not as simple. It is also more easily understood in terms of the loss of amplitude than in terms of the smearing of the response.

For an object at (l, m) relative to the phase-tracking center, the instantaneous phase is $\phi = 2\pi\nu(ul + vm)$, and the phase rate is therefore

$$\frac{d\phi}{dt} = 2\pi\nu \left(\frac{du}{dt} l + \frac{dv}{dt} m \right) . \tag{18–30}$$

Averaging a waveform of frequency f for a time τ reduces the response by a factor sinc $f\tau$, so for $f\tau \ll 1$ the loss in amplitude is $1 - (\pi f\tau)^2/6$. Integrating the visibility data for a time τ_a therefore reduces the amplitude by a factor

$$R_\tau = \frac{I}{I_0} = \text{sinc} \left(\frac{du}{dt} l + \frac{dv}{dt} m \right) \approx 1 - \frac{\pi^2}{6} \left(\frac{du}{dt} l + \frac{dv}{dt} m \right)^2 , \tag{18–31}$$

valid for small τ_a, where I is the peak response to the source in the image, and I_0 is the peak response in the absence of time-average smearing. We saw in Lecture 2 (Eq. 2–30) that, if L_X, L_Y, and L_Z are the coordinate differences for two antennas, the baseline components (u, v, w) are given by

$$\begin{pmatrix} u \\ v \\ w \end{pmatrix} = \frac{1}{\lambda} \begin{pmatrix} \sin H & \cos H & 0 \\ -\sin\delta\cos H & \sin\delta\sin H & \cos\delta \\ \cos\delta\cos H & -\cos\delta\sin H & \sin\delta \end{pmatrix} \begin{pmatrix} L_X \\ L_Y \\ L_Z \end{pmatrix} , \tag{18–32}$$

where H and δ are the hour-angle and declination of the phase reference position and λ is the wavelength corresponding to the center frequency of the receiving system. We can therefore write

$$\frac{du}{dt} = \frac{1}{\lambda} (L_X \cos H - L_Y \sin H) \frac{dH}{dt} \tag{18–33}$$

and

$$\frac{dv}{dt} = \frac{1}{\lambda} (L_X \sin\delta \sin H + L_Y \sin\delta \cos H) \frac{dH}{dt} . \tag{18–34}$$

Substituting these expressions into Equation 18–31 gives an expression for the reduction of amplitude of a point source by time-average smearing on any baseline, as a function of L_X, L_Y, H and δ, provided the reduction is small. The reduction is greatest, for a given baseline, when the apparent diurnal rotation of the sky moves the source at right angles to the fringes associated with that baseline. The reduction is zero when the apparent motion of the source is parallel to the fringes.

2.2. Average effect on an image

For imaging purposes, what is more pertinent is the *average* reduction in amplitude over a 12-hour period. To derive this, we note that $dH/dt = \omega_e$ and use

the following relationships for a given baseline (L_X, L_Y, L_Z):

$$\left(\frac{du}{dt}\right)^2 = \frac{\omega_e^2}{\lambda^2}\left(L_X^2\cos^2 H + L_Y^2\sin^2 H - L_X L_Y \sin 2H\right), \quad (18\text{–}35)$$

$$\left(\frac{dv}{dt}\right)^2 = \frac{\omega_e^2\sin^2\delta}{\lambda^2}\left(L_X^2\sin^2 H + L_Y^2\cos^2 H + L_X L_Y \sin 2H\right), \quad (18\text{–}36)$$

and

$$\frac{du}{dt}\frac{dv}{dt} = \frac{\omega_e^2\sin\delta}{2\lambda^2}\left((L_X^2 - L_Y^2)\sin 2H + 2L_X L_Y\cos 2H\right). \quad (18\text{–}37)$$

Denoting a 12-hour average by $\langle\ \rangle$, and noting that $\langle\sin^2 H\rangle = \langle\cos^2 H\rangle = \frac{1}{2}$ and $\langle\sin 2H\rangle = \langle\cos 2H\rangle = 0$, we have that

$$\left\langle\left(\frac{du}{dt}\right)^2\right\rangle = \frac{\omega_e^2}{2}\frac{L_X^2 + L_Y^2}{\lambda^2}, \qquad \left\langle\left(\frac{dv}{dt}\right)^2\right\rangle = \frac{\omega_e^2\sin^2\delta}{2}\frac{L_X^2 + L_Y^2}{\lambda^2},$$

$$\text{and} \qquad \left\langle\frac{du}{dt}\frac{dv}{dt}\right\rangle = 0, \quad (18\text{–}38)$$

from which we get

$$\langle R_\tau\rangle = \frac{I}{I_0} \approx 1 - \frac{\pi^2}{12}\omega_e^2\tau_a^2\left(l^2 + m^2\sin^2\delta\right)\frac{L_X^2 + L_Y^2}{\lambda^2}. \quad (18\text{–}39)$$

Equation 18–39 applies to a single baseline (L_X, L_Y, L_Z). For an array, we can relate the average of the squared lengths of the equatorial projections of the baseline vectors, $\overline{L_X^2 + L_Y^2}$, to the "dirty" half-power beamwidth $\theta_{\rm HPBW}$ by the expression $\overline{L_X^2 + L_Y^2}/\lambda^2 = \alpha/\theta_{\rm HPBW}^2$. The constant of proportionality α is determined by the baseline distribution and by any tapering (weighting) functions applied to the data. For a synthesis image of a source near the North or South Celestial Pole, the average fractional reduction in amplitude $\overline{\langle R_\tau\rangle}$ produced by time averaging for a source a distance θ from the phase-tracking center can therefore be written in the simple form

$$\overline{\langle R_\tau\rangle} \approx 1 - \frac{\alpha\pi^2}{12}\omega_e^2\tau_a^2\left(\frac{\theta}{\theta_{\rm HPBW}}\right)^2, \quad (18\text{–}40)$$

which is valid in the regime of small intensity losses. We now evaluate the constant α for a few simple cases:

Square coverage, without tapering For square (u, v) coverage of side A (see Eq. 18–14, the beam is given by Equation 18–15, so $\theta_{\rm HPBW}$=1.206/A. For this case, $\overline{L_X^2 + L_Y^2} = A^2\lambda^2/6$, i.e., $\alpha = \frac{1.206^2}{6} = 0.2424$. The average intensity loss factor for a circumpolar point source is therefore

$$\overline{\langle R_\tau\rangle} = 1 - 1.05\times 10^{-9}\left(\frac{\theta}{\theta_{\rm HPBW}}\right)^2\tau_a^2, \quad (18\text{–}41)$$

assuming that the loss due to time-average smearing is small.

Circular coverage, without tapering For circular (u,v) coverage of diameter D, the beam has $\theta_{\rm HPBW} = 1.410/D$. For this case, $\overline{L_X^2 + L_Y^2} = D^2\lambda^2/8$, i.e. $\alpha = \frac{1.410^2}{8} = 0.2485$. The average intensity loss factor for a circumpolar point source is therefore

$$\overline{\langle R_\tau \rangle} = 1 - 1.08 \times 10^{-9} \left(\frac{\theta}{\theta_{\rm HPBW}} \right)^2 \tau_a^2 , \qquad (18\text{–}42)$$

assuming that the loss due to time-average smearing is small.

Circular coverage with Gaussian tapering If the array produces a Gaussian beam with FWHM $\theta_{\rm HPBW}$ (Eq. 18–22), the (u,v) distribution must approximate its transform (Eq. 18–21), so that $\overline{u^2 + v^2} = \gamma^2/\pi^2\theta_{\rm HPBW}^2$ and $\alpha = \gamma^2/\pi^2 = 4(\ln 2)/\pi^2 = 0.2810$. The average intensity loss factor for a circumpolar point source is therefore

$$\overline{\langle R_\tau \rangle} = 1 - 1.22 \times 10^{-9} \left(\frac{\theta}{\theta_{\rm HPBW}} \right)^2 \tau_a^2 , \qquad (18\text{–}43)$$

again assuming that the loss due to time-average smearing is small.

3. Acknowledgments

This lecture draws heavily on previous treatments of these topics by Barry Clark (1981), Rick Perley (1981a) and Dick Thompson (1973; 1982b). We were motivated to add this lecture to the series to collect the results of these earlier treatments, with a few small corrections, into this more widely available format. We hope that in doing so we have amplified them without too much degradation!

References

Bracewell, R. N. 1978, *The Fourier Transform and Its Applications*, Second Edition, McGraw-Hill, New York.

Clark, B. G. 1981, VLA Scientific Memorandum No. 137, NRAO.

Perley, R. A. 1981a, VLA Scientific Memorandum No. 138, NRAO.

Thompson, A. R. 1973, VLA Electronics Memorandum No. 118, NRAO.

Thompson, A. R. 1982b, Lecture No. 5 in *Synthesis Mapping*, A. R. Thompson and L. R. D'Addario, Eds., NRAO (Green Bank, WV).